

PeriodicMFD: A Periodic-based Framework for Multi-source Fault Diagnosis

Jianbo Zheng, Chao Yang, *Member, IEEE*, Tairui Zhang, Bin Jiang, *Member, IEEE*, Xuhui Fan, Xiao-Ming Wu, Haidong Shao, *Senior Member, IEEE*

Abstract—Cross-speed bearing fault diagnosis based on multiple source domains and their data enables high-performance condition monitoring for variable-speed equipment, such as engines and turbines. Current multi-source methods typically employ a fixed-length sampling strategy to construct samples and then align the distributions of these samples from different domains. However, these methods neglect the inherent periodic characteristics of bearing data, resulting in incomplete or redundant periodic features in the samples. To address this challenge, we propose a periodic-based framework, PeriodicMFD, for multi-source cross-speed fault diagnosis, which ensures complete periodic information. Our PeriodicMFD framework begins with a periodic sampling strategy designed to construct periodic samples that effectively capture periodic features while maintaining their periodic integrity. Nevertheless, periodic samples from different domains exhibit inconsistencies at both the sample and domain levels. To reconcile these inconsistencies, we introduce sample-level matching to address inconsistencies in feature dimensions and fault patterns among samples from various domains. Additionally, we propose domain-level alignment to handle inconsistencies in space and distribution across different domains. Extensive experiments across three datasets highlight the effectiveness of the PeriodicMFD framework, with a stable average accuracy of 99.55%.

Index Terms—Domain adaptation, periodic sampling, multi-source fault diagnosis.

I. INTRODUCTION

BEARING faults, which can be identified by abnormal vibrations, are common in mechanical equipment such as engines, wind turbines, and machine tools. Intelligent diagnosis of bearing faults by analyzing vibration data is of significant research value [1]–[6]. However, the distribution of bearing data varies significantly across different operating speeds, with each speed being considered a distinct

Jianbo Zheng, Chao Yang, Tairui Zhang, and Bin Jiang are with the College of Computer Science and Electronic Engineering, Hunan University, Changsha, China. Xuhui Fan is with the School of Computing, Macquarie University, Australia. Xiao-Ming Wu is with the School of Computer Science and Engineering, Sun Yat-sen University, China. Haidong Shao is with the College of Mechanical and Vehicle Engineering, Hunan University, Changsha, China. Corresponding authors: Chao Yang (yangchaoed@hnu.edu.cn) and Haidong Shao (hdshao@hnu.edu.cn).

This work is an extended version of the conference paper titled “A Rolling Bearing Fault Diagnosis Method Using Multi-Sensor Data and Periodic Sampling,” which was presented at the 2022 IEEE International Conference on Multimedia and Expo held in Taipei, Taiwan, from July 18 to 22, 2022.

This work was supported by the National Natural Science Foundation of China under Grant No.62072169 and No.52275104, the China Scholarship Council Program under Grant No.202306130083, and the Postgraduate Scientific Research Innovation Project of Hunan Province under Grant No.QL20230099.

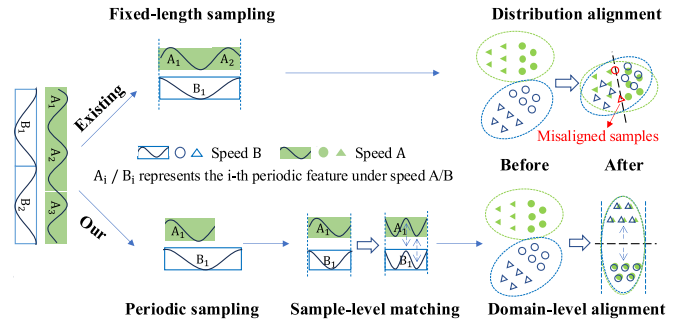


Fig. 1. Framework comparison between existing methods and our proposed PeriodicMFD method. The existing methods include fixed-length sampling and distribution alignment. In contrast, our PeriodicMFD method employs a systematic three-step process: Periodic sampling, sample-level matching, and domain-level alignment.

domain. This variability leads to decreased performance of deep learning methods under cross-speed conditions [7]–[9]. Consequently, the limited fault knowledge from a single source domain has shifted the focus towards multi-source cross-speed fault diagnosis, utilizing multi-source unsupervised domain adaptation techniques to enhance diagnostic performance by integrating knowledge from multiple domains [10].

Existing multi-source cross-speed fault diagnosis methods are divided into two steps. First, a fixed-length sampling strategy is used to construct samples of uniform length (feature dimension) from vibration data across various domains, such as 1024, 2048, or other empirically determined static values [11]. Then, statistical functions or adversarial neural networks are used to align the distributions of these samples from different domains [12], [13]. Despite the progress made by existing methods [14]–[16], they often ignore the inherent periodic characteristics of bearing data, resulting in incomplete or redundant periodic features in fixed-length samples. To address this challenge, this paper introduces a periodic-based framework termed PeriodicMFD, as illustrated in Fig. 1. Leveraging the intrinsic periodic characteristics of bearing data, the PeriodicMFD framework effectively constructs periodic samples and facilitates consistent alignment of these periodic samples across diverse domains, thereby significantly enhancing multi-source cross-speed fault diagnosis performance.

Our PeriodicMFD framework begins with a periodic sampling strategy aiming at constructing periodic samples that effectively capture periodic features while ensuring their periodic integrity. Given that the vibration data of bearings is

generated by their rotation, it is considered that any abnormal data also exhibit periodic characteristics consistent with the rotation period [17]. Consequently, we set the sample length to the number of sampling points recorded during one complete rotation period, ensuring that each periodic sample has a complete periodic feature. Unfortunately, this periodic sampling strategy leads to inconsistencies at both the sample and domain levels. At the sample level, sample inconsistencies manifest in feature dimensions and fault patterns among samples constructed from various domains, which are correlated with the bearing's rotational speed. At the domain level, domain inconsistencies arise in sample spaces and distributions across different domains, with each domain exhibiting its own unique sample space and distribution.

To reconcile these inconsistencies at both the sample and domain levels, our PeriodicMFD framework proposes sample-level matching and domain-level alignment. The sample-level matching focuses on resolving sample inconsistencies through two critical processes: first, scaling periodic samples to ensure consistent feature dimensions while preserving their periodic integrity; and second, employing a pattern matcher to match fault patterns among periodic samples. In parallel with sample-level matching, domain-level alignment is introduced to mitigate domain inconsistencies through two key steps: first, utilizing distance-based space alignment to reduce the distance between sample spaces of different domains; and second, proposing uncertainty-based distribution alignment to implicitly align the sample distributions across domains by expanding the distinction between classes.

This paper proposes the PeriodicMFD framework, which aims to achieve consistent alignment of periodic features with complete periodic information to facilitate multi-source cross-speed fault diagnosis. Extensive experiments conducted on eighteen multi-source cross-speed tasks across three datasets demonstrate the effectiveness of the PeriodicMFD framework, yielding a stable average accuracy of 99.55%.

The contributions of this work are summarized as follows:

- We extend our previously proposed periodic sampling strategy for deep learning-based fault diagnosis [17] to tackle the multi-source cross-speed fault diagnosis. This study is the first to systematically leverage the periodic features while ensuring their periodic integrity.
- We propose sample-level matching and domain-level alignment to ensure consistent alignment of periodic features across diverse domains, effectively resolving inconsistencies arising from periodic sampling.
- Extensive experiments on three datasets demonstrate the effectiveness of our proposed PeriodicMFD framework, and all code will be accessible on GitHub¹.

The remainder of this paper is organized as follows: Section II reviews related works. Section III defines the tasks and provides detailed descriptions of the PeriodicMFD framework. Section IV elaborates on the experiment settings across three datasets. Section V presents and analyzes the experimental results. Finally, Section VI offers conclusions.

II. RELATED WORK

For cross-speed fault diagnosis, multi-source domain generalization extracts domain-invariant knowledge exclusively from multiple labeled source domains [18]. Conversely, multi-source unsupervised domain adaptation (MUDA) not only leverages multiple labeled source domains but also incorporates unlabeled target domains, leading to improved performance outcomes [19]. In this paper, we succinctly delineate existing MUDA methodologies relevant to cross-speed fault diagnosis into two distinct phases.

The first phase, termed **sample construction**, involves the transformation of raw vibration data into structured samples suitable for training artificial intelligence algorithms. Presently, the predominant sampling strategy employed is fixed-length sampling, which utilizes a sliding window to construct one-dimensional samples of unified length [11]. Additionally, some methods employ Fast Fourier Transform (FFT) or Short-Time Fourier Transform (STFT) techniques to convert these one-dimensional fixed-length samples into two-dimensional representations, thereby enhancing model performance through mature image processing techniques [20]. However, this transformation considerably escalates the computational cost of the models. Regrettably, existing MUDA methods ignore the periodic characteristics of bearing vibration data, resulting in incomplete or redundant periodic features in the fixed-length samples.

The second phase, termed **distribution alignment**, involves utilizing an appropriate network architecture to automatically extract domain-invariant fault features from one-dimensional or two-dimensional samples across multiple domains. Subsequently, it addresses the challenge of distribution discrepancies among samples from different domains by using measurement functions such as Maximum Mean Discrepancy (MMD), Multiple Kernel MMD (MK-MMD) [21], Joint MMD (JMMD) [12], or Generative Adversarial Networks (GANs). In general, two optimizations can be used to enhance domain distribution alignment. The first focuses on refining the network architecture responsible for feature extraction. For instance, Wu et al. propose a knowledge dynamic matching unit-guided multi-source domain adaptation network with an attention mechanism, which converts the multi-source task into multiple single-source tasks and introduces knowledge dynamic matching units for domain-invariant feature extraction [22]. Xu et al. propose an IFDS method, which constructs a cross-domain discriminator for each source domain by considering the differences between multiple sources and obtains domain-invariant features through adversarial neural network [23]. The second involves optimizing the loss function that guides the model to achieve better domain distribution alignment. For example, Yu et al. present the MSIDA-Net method, which integrates a domain attribute loss function with the local MMD metric to extract domain-invariant features [24]. Cao et al. implemented a decision voting mechanism to effectively distinguish the varying contributions of different source domain information within the loss function [25]. Nonetheless, these methods also neglect the periodic characteristics of bearing vibration data, resulting in inconsistent distribution alignment.

¹<https://github.com/IWantBe/PeriodicMFD>

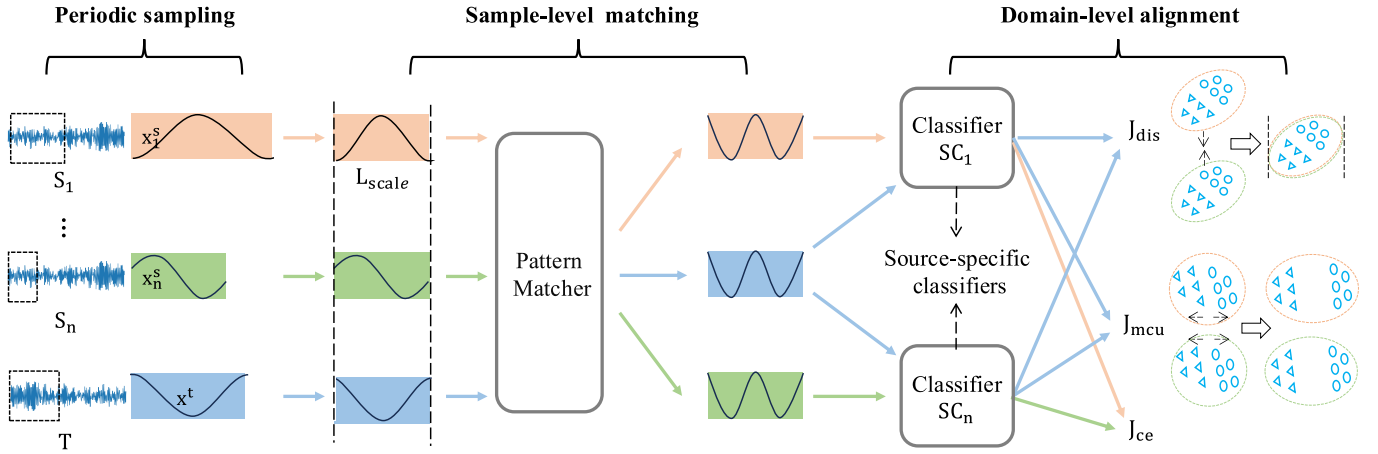


Fig. 2. The Framework of PeriodicMFD. PeriodicMFD comprises three key components: First, periodic sampling is proposed to construct periodic samples with complete periodic features. Second, sample-level matching is introduced to address inconsistencies among periodic samples by matching their feature dimensions and fault patterns. Finally, domain-level alignment is implemented to handle domain inconsistencies by minimizing the distance between sample spaces (J_{dis}) and implicitly aligning the sample distributions based on minimal uncertainty (J_{mcu}).

In this paper, leveraging the intrinsic periodic characteristics of bearing data, we propose the PeriodicMFD framework to ensure complete periodic information. First, periodic sampling is proposed to construct periodic samples that effectively capture periodic features while maintaining their periodic integrity. Subsequently, to address the inconsistencies arising from periodic sampling at both the sample and domain levels, we introduce sample-level matching and domain-level alignment to ensure consistent alignment of periodic samples across diverse domains. Ultimately, the complete periodic features and consistent alignment synergistically empower the PeriodicMFD framework to achieve optimal cross-speed fault diagnosis performance.

III. THE PERIODICMFD FRAMEWORK

To effectively leverage the bearing periodic features, we propose the PeriodicMFD framework for enhanced multi-source cross-speed fault diagnosis, as illustrated in Fig. 2.

Task Definition: Consider n labeled source domains $\{S_1, \dots, S_n\}$ and an unlabeled target domain T . Each source domain S_j is defined as a set of pairs $\{x^{s_j}, y^{s_j}\}$, where x^{s_j} represents the sample features and y^{s_j} indicates the corresponding labels in the j -th source domain, for $j \in \{1, \dots, n\}$. The target domain T consists solely of sample features, represented as $\{x^t\}$, where x^t are the features without associated labels in the target domain. Multi-source unsupervised domain adaptation for cross-speed fault diagnosis aims to collaboratively train a predictive function $f(\cdot)$ using n labeled source domains and an unlabeled target domain T . Upon completion of the training process, the trained function $f(\cdot)$ is deployed to accurately predict the labels of the unlabeled sample features x^t within the target domain.

A. Periodic Sampling

The bearing vibration data exhibits intrinsic periodic characteristics, with a period that corresponds to the rotation period of the bearing. In this part, we propose a periodic

sampling strategy designed to construct periodic samples that effectively capture periodic features while maintaining their periodic integrity. This sampling strategy ensures that all constructed samples encompass complete periodic features, thereby enhancing multi-source cross-speed fault diagnosis.

Based on revolutions per minute (RPM) and sampling frequency f , we can determine the number of sampling points n within a bearing's rotation period, as described in our previous work [17]. The formula is as follows:

$$n = \frac{60 \times f}{\text{RPM}}. \quad (1)$$

Then, since the number of sampling points n within a bearing rotation period varies with the rotation speed, the sampling points n at different rotation speeds must be scaled to ensure that they have consistent feature dimensions. In this paper, we simply address the inconsistency in feature dimensions by scaling them to a predefined dimension L_{scale} , with specific details provided in Section III-B. Based on n and L_{scale} , we can calculate the feature dimension L_{periodic} of periodic samples as follows:

$$L_{\text{periodic}} = \left\lceil \frac{n}{L_{\text{scale}}} \right\rceil \times L_{\text{scale}}, \quad (2)$$

where $\lceil \cdot \rceil$ represents the upper bound.

Next, the number of samples for each category is predefined as m . Utilizing the total number of sample points N , the feature dimension L_{periodic} , and the specified number of samples m , we calculate the sliding stride S for periodic sampling as follows:

$$S = \begin{cases} \left\lceil \frac{N - L_{\text{periodic}}}{m-1} \right\rceil, & \text{if } S > L_{\text{periodic}}, \\ S = L_{\text{periodic}}; & \\ \left\lfloor \frac{N - L_{\text{periodic}}}{m-1} \right\rfloor, & \text{if } S \leq L_{\text{periodic}}. \end{cases} \quad (3)$$

Here, $\lfloor \cdot \rfloor$ represents the lower bound.

Finally, following our previous work [17], we employ a sliding window with a window length of L_{periodic} and a sliding stride of S to construct periodic samples. This process

results in a periodic sample set encompassing K categories, as detailed below:

$$\text{Sample}_{\text{periodic}} = \{(\mathbf{x}_i, \mathbf{y}) \mid i \in [1, m], y \in [1, K]\}, \quad (4)$$

where \mathbf{x}_i is the feature of the i -th periodic sample, \mathbf{y} is the category label of \mathbf{x}_i with a total of K categories, and the feature dimension, or sample length, of \mathbf{x}_i is L_{periodic} .

Although periodic sampling constructs periodic samples that effectively capture periodic features while ensuring their periodic integrity, it introduces inconsistencies at both the sample and domain levels during performing multi-source cross-speed fault diagnosis.

B. Sample-level Matching

In this part, we propose sample-level matching to address sample inconsistencies in feature dimensions and fault patterns across different domains. We begin with introducing the feature scaling process to ensure consistent feature dimensions. Subsequently, we implement pattern matching to match fault patterns across samples effectively.

Feature scaling: To address the inconsistencies in feature dimensions across samples from different domains, we simply scale these samples to a consistent feature dimension. First, the scaling factor θ is calculated using n and L_{scale} as follows:

$$\theta = \left\lceil \frac{n}{L_{\text{scale}}} \right\rceil. \quad (5)$$

Then, based on the scaling factor θ , the scaling for periodic samples \mathbf{x}_i is defined as follows:

$$\bar{\mathbf{x}}_{i_g} = \frac{1}{\theta} \sum_{l=1}^g \mathbf{x}_{i_{(g-1)\theta+l}}, \quad (6)$$

where $\bar{\mathbf{x}}_{i_g}$ is the g -th sampling point of the i -th scaled sample, and $g \in [1, L_{\text{scale}}]$.

Last, the scaled sample set with consistent feature dimensions is obtained.

$$\text{Sample}_{\text{scale}} = \{(\bar{\mathbf{x}}_i, \mathbf{y}), i \in [1, m], y \in [1, K]\}, \quad (7)$$

where $\bar{\mathbf{x}}_i$ is the feature of the i -th scaled sample, \mathbf{y} is the category label of $\bar{\mathbf{x}}_i$, and the dimension of all scaled samples $\bar{\mathbf{x}}$ are L_{scale} .

Pattern matching: To address the inconsistencies in fault patterns across samples, we implement a pattern matcher that employs multiple convolutional and pooling layers, specifically employing two layers in this paper. This matcher is designed to identify consistent fault patterns that are independent of rotational speeds, thereby enhancing the matching of these patterns across samples.

In brief, we achieve sample-level matching through feature scaling and pattern matching. This process addresses inconsistencies between samples and facilitates the resolution of subsequent domain inconsistency issues.

C. Domain-level Alignment

Although sample-level matching can address inconsistencies among samples, challenges persist regarding space and distribution inconsistencies across different domains. To address these domain inconsistencies, we propose domain-level alignment, which includes both distance-based space alignment and uncertainty-based distribution alignment.

Distance-based space alignment: We first design n source-specific classifiers SC , each corresponding to one of the n source domains. Each classifier consists of two fully connected layers and is trained on samples from both the target domain and its respective source domain. Given that each classifier is trained on data from a single source domain, discrepancies may arise in their predictions for target domain samples. These discrepancies reflect variations in the projections of target domain samples across the source domain spaces, which can be viewed as space inconsistencies.

Next, we define the domain distance loss term J_{dis} , which represents the average distance between the predictions of target domain samples from various source-specific classifiers. This term quantifies the differences in prediction results (spaces) across various domains. Minimizing J_{dis} encourages all source-specific classifiers to produce similar predictions based on their respective source knowledge, thereby alleviating space inconsistencies among source domains and achieving effective space alignment.

The formula for calculating J_{dis} is as follows:

$$J_{\text{dis}} = \frac{2}{n^2 - n} \sum_{j=1}^n \sum_{i=1, i \neq j}^n \sum_{l=1}^m |SC_j(\mathbf{x}_l^t) - SC_i(\mathbf{x}_l^t)|, \quad (8)$$

where $SC_j(\mathbf{x}_l^t)$ is the predicted value of the j -th source-specific classifier for the l -th sample in the target domain, and $|.|$ represents the absolute value.

Uncertainty-based distribution alignment: We start with introducing a trainable weight layer, $\omega = [\omega_1, \dots, \omega_n]$, designed to adaptively capture the influence of each source domain on the final prediction, subject to the constraint that $\sum_{i=1}^n \omega_i = 1$. Subsequently, to handle distribution inconsistencies between the target domain and the source domains, we propose a multi-source class uncertainty loss term J_{mcu} . This term quantifies the degree of uncertainty across multiple classes for samples in the target domain, and implicitly facilitates the distribution alignment between the source domains and target domain.

The formula for calculating J_{mcu} is as follows:

$$J_{\text{mcu}} = \sum_{j=1}^n \omega_j MCC_j(\mathbf{y}^t), \quad (9)$$

$$MCC(y) = \frac{1}{|C|} \sum_{j=1}^{|C|} \sum_{i \neq j}^{|C|} \left| \frac{\mathbf{y}_{j,i}^T \mathbf{y}_{i,i}}{\sum_{k=1}^{|C|} \mathbf{y}_{j,k}^T \mathbf{y}_{i,k}} \right|, \quad (10)$$

where $MCC_j(\mathbf{y}^t)$ is the class uncertainty value of the target domain sample on the j -th trained source-specific classifier. ω_j is the weight of the j -th source domain. $|C|$ is the number of categories in the source domain, and $\mathbf{y}_{j,i}^T \mathbf{y}_{i,i}$ is a coarse estimation of the class uncertainty, which measures the

probability that samples are simultaneously classified into both class j and class i . y_{ji} represents the probabilities of samples that come from the i -th class.

By minimizing J_{mcu} , we increase the probability differentiation for target domain samples being classified into distinct classes, effectively mitigating the prevalent phenomenon of class confusion [26] that arises from high uncertainty in existing distance-based distribution alignment methods. Furthermore, reducing class uncertainty also alleviates distribution inconsistencies between the target and source domains by implicitly facilitating effective distribution alignment [26].

D. Model Training

To achieve optimal multi-source cross-speed fault diagnosis, we propose a total loss function, denoted as J_{total} , which supervises the training of the PeriodicMFD framework that integrates periodic sampling, sample-level matching, and domain-level alignment. Specifically, J_{total} comprises three key components: the multi-source cross-entropy loss term J_{ce} , the multi-source class uncertainty loss term J_{mcu} , and the domain distance loss term J_{dis} . The formulation of the total loss J_{total} is defined as follows:

$$J_{total} = J_{ce} + \gamma(J_{mcu} + J_{dis}), \quad (11)$$

where γ serves as an equilibrium parameter that changes as the number of epochs progresses, facilitating a balance between the components of the total loss function. For simplicity, we assume equal importance for J_{mcu} and J_{dis} .

The loss term J_{ce} represents the weighted sum of cross-entropy losses for samples from n source domains, evaluated by their respective source-specific classifiers. It is formulated as follows:

$$J_{ce} = - \sum_{j=1}^n \omega_j \sum_{i=1}^m p^{s_j}(\mathbf{x}_i^{s_j}) \log (q^{s_j}(\mathbf{x}_i^{s_j})), \quad (12)$$

where n denotes the number of source-specific classifiers within our PeriodicMFD framework, m represents the number of samples in \mathbf{x}^{s_j} . ω_j is the weight assigned to the j -th source domain. Here, $p^{s_j}(\mathbf{x}_i^{s_j})$, $q^{s_j}(\mathbf{x}_i^{s_j})$ are the ground truth and predicted distributions, respectively, for the i -th sample from the j -th source domain as evaluated by the j -th source-specific classifier.

The parameter of γ is computed as follows:

$$\gamma = \frac{2}{\left(1 + e^{-10 \frac{\text{epoch}}{\text{Epochs}}}\right)} - 1, \quad (13)$$

where epoch denotes the current epoch number, and Epochs represents the total number of epochs.

IV. EXPERIMENT SETTINGS

A. Datasets Description

To evaluate the effectiveness of our proposed PeriodicMFD framework, comprehensive experiments are conducted on three extensively studied datasets: the JiangNan University (JNU) dataset, the Case Western Reserve University (CWRU) dataset, and the HUSTbearing (HUST) dataset [18], [27], [28].

In the JNU dataset, vibration data is collected at three distinct rotational speeds: 600 RPM, 800 RPM, and 1000 RPM, with a sampling frequency of 50 kHz. Each speed data encompasses four types of vibration data: Normal, Outer Ring (OR) fault, Inner Ring (IR) fault, and Ball fault. In the CWRU dataset, the “48K drive end bearing fault data” with a sampling frequency of 48kHz is used, which includes bearing vibration data recorded at four different speeds: 1797 RPM, 1772 RPM, 1750 RPM, and 1730 RPM. Each RPM category comprises ten types of data, including one normal sample and nine fault samples, which vary by fault types (OR, IR, or Ball) or fault diameters (7, 14, or 21 mils). For the HUST dataset, data is collected at rotational speeds of 3900 RPM (65 Hz), 4200 RPM (70 Hz), and 4800 RPM (80 Hz), with a sampling frequency of 25.6 kHz. Each RPM category includes nine types of data, comprising one normal sample and eight fault samples that differ by fault types (OR, IR, Ball, or combination fault) or severity (severe or medium).

B. Tasks Description

The multi-source cross-speed fault diagnosis task, denoted as $(S_1, S_2) \rightarrow T$, involves training the model using labeled samples from two source domains (speeds) S_1 and S_2 , alongside unlabeled samples from target domain T . The model’s performance is subsequently evaluated using unlabeled samples from T .

We establish twelve multi-source cross-speed tasks (C1 to C12) based on the four rotational speeds available in the CWRU dataset. Additionally, we define three multi-source cross-speed tasks (J1 to J3) using the three speeds from the JNU dataset, and three more tasks (H1 to H3) derived from the three speeds in the HUST dataset. As detailed in Section V-D, the recommended scaled sample lengths for these tasks are $L_{\text{scale}}^{\text{CWRU}} = 420$, $L_{\text{scale}}^{\text{JNU}} = 500$ and $L_{\text{scale}}^{\text{HUST}} = 400$, respectively. A comprehensive summary of these eighteen multi-source cross-speed fault diagnosis tasks and their corresponding scaled sample lengths is presented in Table I.

C. Implementation Details

In this paper, the deep learning framework PyTorch 2.0.1 is applied to build the model. All experimental methods are executed ten times to mitigate the impact of randomness. For the three datasets under consideration, the number of samples per class, denoted as m , is consistently set at 500. Furthermore, the vibration data from the target domain is partitioned into training and testing sets with a ratio of [0.9, 0.1]. Specifically, the CWRU dataset comprises 4500 samples for training and 500 samples for testing. The JNU dataset consists of 1800 samples for training and 200 samples for testing. Finally, the HUST dataset includes 4050 samples for training and 450 samples for testing. A comprehensive overview of the predefined hyper-parameters is presented in Table II.

V. EXPERIMENT RESULTS

To evaluate the effectiveness of the PeriodicMFD framework, we develop nine distinct methods, as summarized in

TABLE I
MULTI-SOURCE CROSS-SPEED TASKS

Datasets	L_{scale}	Tasks				
JNU	$L_{\text{scale}}^{\text{JNU}} = 500$	J1: (600, 800)→1000 C1: (1797, 1772)→1750	J2: (600, 1000)→800 C2: (1797, 1772)→1730	J3: (800, 1000)→600 C3: (1797, 1750)→1772	C5: (1797, 1730)→1772 C6: (1797, 1730)→1750	C9: (1772, 1750)→1797 C12: (1750, 1730)→1772
CWRU	$L_{\text{scale}}^{\text{CWRU}} = 420$	C4: (1797, 1750)→1730 C7: (1772, 1750)→1797 C10: (1772, 1730)→1750	C8: (1772, 1750)→1730 C11: (1750, 1730)→1797	H2: (3900, 4800)→4200	H3: (4200, 4800)→3900	
HUST	$L_{\text{scale}}^{\text{HUST}} = 400$	H1: (3900, 4200)→4800				

TABLE II
HYPER-PARAMETERS

Name	Value	Name	Value
Epochs	100	Filters	32
Learning rate	10^{-3}	Kernel_size	21
Batch_size	32	Strides(Conv1D)	1
Activation	ReLU	Pool_size	2
Padding(Conv1D)	same	Padding(Pool1D)	same

Table III. These methods include our PeriodicMFD method, five recent methods for overall performance comparison (MCC [26], MK-MMD [29], JMMD [29], MSSA [30], and TSMDA [25]), as well as three ablation methods (Wo/ PS, Wo/ SM, and Wo/ DA) designed to isolate the contributions of each component.

Three ablation methods are defined as follows: **(1) W/o PS:** This method omits the periodic sampling component from the PeriodicMFD framework. The W/o PS method begins with a fixed-length sampling strategy to construct fixed-length samples. It then performs sample-level matching and domain-level alignment on these fixed-length samples. **(2) W/o SM:** This method eliminates the sample-level matching component from the PeriodicMFD framework. The W/o SM method starts with periodic sampling to construct periodic samples x . Subsequently, the first L_{scale} sampling points of each periodic sample are truncated to form scaled samples \bar{x} with consistent feature dimensions. These scaled samples \bar{x} then undergo pattern matching and domain-level alignment. **(3) W/o DA:** This method excludes the domain-level alignment component from the PeriodicMFD framework. The W/o PS method initiates with periodic sampling to construct periodic samples. Following this, it conducts sample-level matching and utilizes the MK-MMD loss term to align the sample distributions between various domains.

A. Overall Performance Comparison

Table IV presents the average accuracy results for the PeriodicMFD method compared to five recent methods across eighteen multi-source tasks in three datasets. The average accuracies for MCC, MK-MMD, JMMD, MSSA, TSMDA, and our proposed PeriodicMFD method are 93.08%, 95.88%, 95.58%, 87.52%, 89.05%, and 99.55%, respectively, with corresponding standard deviations (SD) of 6.03, 5.30, 6.41, 41.35, 11.98, and 0.49. The PeriodicMFD method exhibits substantial improvements over MCC, MK-MMD, JMMD, MSSA, and TSMDA, achieving increases in average accuracy

of 6.47%, 3.67%, 3.97%, 12.03%, and 10.50%, respectively, alongside reductions in SD of 5.54, 4.81, 5.92, 9.51, and 11.49. This indicates its enhanced performance in multi-source cross-speed fault diagnosis.

The superior performance of the PeriodicMFD method can be attributed to the following factors. Existing methods predominantly utilize a fixed-length sampling strategy for sample construction, followed by distribution alignment across different domains. However, they often neglect the periodic features inherent in bearing data, resulting in a mismatch of periodic fault patterns when aligning fixed-length samples from different domains with varying rotational speeds, thus compromising the quality of distribution alignment.

In contrast, the PeriodicMFD method employs a periodic sampling strategy to construct periodic samples with feature dimensions corresponding to one complete rotation period, thereby leveraging the inherent periodic characteristics of bearing data. This approach ensures that each sample accurately encapsulates periodic features of a complete rotation period, thereby facilitating the alignment of periodic features across different domains. Additionally, the PeriodicMFD method integrates sample-level matching with domain-level alignment to address inconsistencies arising from periodic sampling, thereby achieving consistent alignment of periodic features across diverse domains, significantly enhancing distribution alignment and achieving the optimal overall performance.

B. Ablation Analysis

The accuracy results for the three ablation methods and our PeriodicMFD method on eighteen multi-source cross-speed tasks are presented in Table V. The average accuracies of 95.39% for W/o PS, 93.88% for W/o SM, 87.20% for W/o DA, and 99.55% for our PeriodicMFD method, with corresponding standard deviations (SDs) of 4.75, 7.92, 11.92, and 0.49, respectively. Notably, the PeriodicMFD method achieves both the highest average accuracy and the lowest SD across three datasets, indicating its superiority.

(1) The W/o PS method, which employs fixed-length sampling, demonstrates an average accuracy 4.16% lower than the PeriodicMFD method. This reduction is attributed to fixed-length sampling ignoring the inherent periodicity of bearing vibration data. In contrast, the PeriodicMFD method adopts the periodic sampling strategy that effectively leverages these periodic features, thus facilitating consistent distribution alignment.

(2) The W/o SM method, which eliminates sample-level matching, exhibits an average accuracy 5.67% lower than the

TABLE III
DESCRIPTION OF EXPERIMENTAL METHODS

Experiments		Method	Sampling strategy	Domain distribution alignment	
Overall comparison	MCC [26]	Fixed-length sampling		Traditional CNN architecture & MCC loss term	
	MK-MMD [29]			Two stage architecture & MK-MMD loss term	
	JMMD [29]			Two stage architecture & JMMD loss term	
	MSSA [30]			MSSA architecture & LMMD loss term	
	TSMDA [25]			TSMDA architecture & LMMD loss term	
Ablation comparison	Our PeriodicMFD	Periodic sampling		Sample-level matching	Domain-level alignment
	W/o PS			✓	✓
	W/o SM			✗	✓
	W/o DA			✓	✗

TABLE IV
ACCURACY OF OVERALL COMPARISON METHODS

Task	MCC	MK-MMD	JMMD	MSSA	TSMDA	PeriodicMFD
C1	94.44	97.54	97.65	90.31	92.64	99.35
C2	85.33	95.65	95.35	84.1	96.53	99.25
C3	98.63	99.06	99.02	90.29	94.88	99.79
C4	89.85	96.71	96.63	82.92	98.28	99.88
C5	95.29	98.25	98.29	89.27	93.84	99.21
C6	88.56	95.77	96.13	86.94	92.71	98.58
C7	92.83	90.35	89.29	75.71	92.86	100
C8	91.04	97.9	98.21	89.42	97.38	100
C9	87.94	88.5	88.6	75.94	94.17	98.96
C10	93.69	98.04	98.17	91.63	94.69	98.77
C11	77.17	93.73	93.5	60.1	91.15	100
C12	95.81	98.25	98.69	89.58	93.8	99.44
J1	100	99.53	99.64	98.7	85.63	99.95
J2	100	99.95	99.69	98.59	93.39	100
J3	95.05	99.95	99.95	98.85	81.88	100
H1	90.31	78.91	73.66	87.54	54.24	98.97
H2	99.75	97.83	97.92	96.83	61.88	99.8
H3	99.82	99.96	100	88.64	92.97	100
Accuracy	93.08	95.88	95.58	87.52	89.05	99.55
SD	6.03	5.30	6.41	9.60	11.98	0.49

PeriodicMFD method. This decline stems from two factors: first, periodic samples derived from the periodic sampling strategy exhibit significant inconsistencies at the sample level, particularly regarding feature dimensions and fault patterns. Second, truncating periodic samples leads to mismatches in periodic features, akin to issues in fixed-length sampling. Conversely, the PeriodicMFD method applies feature scaling to ensure consistency in feature dimensions while preserving the integrity of periodic features. Subsequently, it extracts cross-speed fault patterns through pattern matching, further enhancing distribution alignment.

(3) The W/o DA method, which excludes domain-level alignment, shows an average accuracy 12.35% lower than the PeriodicMFD method. This discrepancy can be explained as follows: the W/o DA method only utilizes the MK-MMD loss term for domain distribution alignment without adequately addressing the inconsistencies in feature spaces among periodic samples from different domains. Additionally, the MK-MMD loss term is susceptible to class confusion issues arising from high uncertainty. In contrast, the PeriodicMFD method first mitigates space inconsistencies through distance-based space alignment (J_{dis}), followed by the introduction of an uncertainty-based distribution alignment (J_{mcu}) to implicitly achieve more effective distribution alignment.

TABLE V
ACCURACY OF ABLATION COMPARISON METHODS

Task	W/o PS	W/o SM	W/o DA	PeriodicMFD
C1	97.23	93.21	72.46	99.35
C2	91.63	81.50	78.79	99.25
C3	98.96	96.54	97.81	99.79
C4	92.00	86.35	89.92	99.88
C5	97.94	96.71	76.98	99.21
C6	91.77	95.42	96.06	98.58
C7	89.00	89.54	95.79	100
C8	97.96	95.44	99.25	100
C9	88.52	89.77	94.96	98.96
C10	96.92	98.25	97.13	98.77
C11	84.33	70.29	83.69	100
C12	98.96	98.38	80.73	99.44
J1	100.00	99.84	95.42	99.95
J2	100.00	99.90	93.39	100
J3	94.27	99.22	96.77	100
H1	99.93	99.46	58.66	98.97
H2	97.63	99.98	68.59	99.8
H3	100.00	99.98	93.21	100
Accuracy	95.39	93.88	87.20	99.55
SD	4.75	7.92	11.92	0.49

C. Visualization Analysis

To intuitively illustrate the effectiveness of our PeriodicMFD method, we present visualization results derived from t-distributed Stochastic Neighbor Embedding (t-SNE) in Fig. 3. This visualization facilitates a comparative analysis of the outcomes from the W/o PS, W/o SM, W/o DA, MCC, TSMDA and PeriodicMFD methods within the multi-source cross-speed task C7.

As depicted in Fig. 3, the W/o PS method, which employs fixed-length sampling, the W/o SM method that eliminates sample-level matching, and the W/o DA method that excludes domain-level alignment, along with MCC and TSMDA, all encounter significant challenges characterized by indistinct classification boundaries. In stark contrast, our PeriodicMFD method effectively integrates periodic sampling, sample-level matching, and domain-level alignment, thereby leveraging the intrinsic periodic features of bearing data. This comprehensive approach results in clearly delineated classification boundaries among distinct categories.

D. The effect of scaled sample length on model performance

The scaled sample length L_{scale} of samples not only affects the number of model parameters (more parameters result in increased training time) but also influences the diagnostic

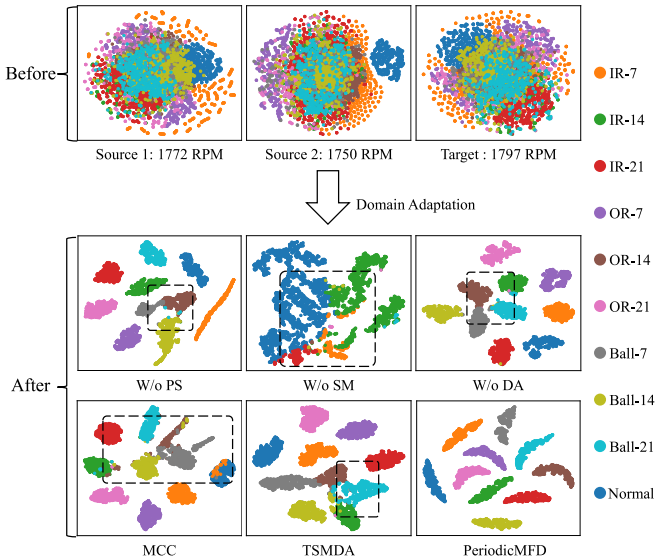


Fig. 3. The t-SNE visual analysis for our PeriodicMFD method. The top section illustrates the sample distribution for the source domain at 1772 RPM, the source domain at 1750 RPM, and the target domain at 1799 RPM. The middle section displays the t-SNE results following domain adaptation for the three ablation methods: W/o PS, W/o SM, and W/o DA. Finally, the bottom section presents the t-SNE results of MCC method, TSMDA method and our proposed PeriodicMFD method. Additionally, the deficiencies that persist after domain adaptation using the W/o PS, W/o SM, W/o DA, MCC, and TSMDA methods are highlighted within the black dashed boxes.

accuracy of the model. In the multi-source task C7 of the CWRU dataset, we investigate the impact of varying scaled sample lengths on both model parameters and diagnostic accuracy. The experimental results are illustrated in Fig. 4.

For scaled sample lengths of 105 and 210, the model achieves diagnostic accuracies of 49.38% and 89.96%, respectively, with corresponding model parameters of $211K$ and $376K$. However, for scaled sample lengths of 420, 630, 840, 1050, and 1260, the diagnostic accuracy consistently reaches 100%, with model parameters of $717K$, $1050K$, $1389K$, $1722K$, and $2061K$, respectively. Furthermore, as the number of model parameters increases, the required training time also gradually rises. Based on the analysis of the results presented in Fig. 4, we conclude that setting the scaled sample length to $L_{\text{scale}}^{\text{CWRU}} = 420$ for tasks within the CWRU dataset effectively minimizes both model parameters and training time without compromising diagnostic accuracy. Similarly, for tasks within the JNU and HUST datasets, the recommended scaled sample lengths are $L_{\text{scale}}^{\text{JNU}} = 500$ and $L_{\text{scale}}^{\text{HUST}} = 400$, respectively.

VI. CONCLUSION

In this paper, we present the PeriodicMFD framework for multi-source cross-speed fault diagnosis, which leverages periodic characteristics of bearing data to ensure consistent alignment of periodic features across diverse domains. PeriodicMFD framework begins with a periodic sampling strategy to construct periodic samples with complete periodic features. Subsequently, it incorporates sample-level matching and domain-level alignment to address inconsistencies at both the sample and domain levels. Experimental results obtained from

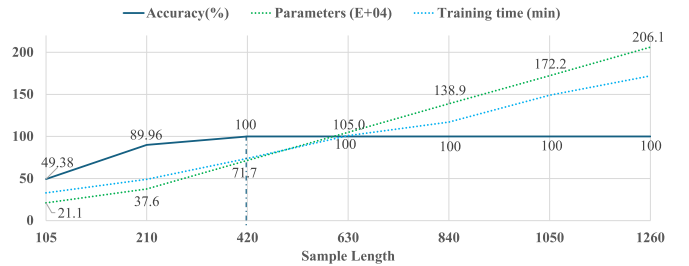


Fig. 4. The impact of sample length on model performance.

three distinct datasets substantiate the superiority of the PeriodicMFD framework, which achieves optimal performance through the integration of periodic sampling, sample-level matching, and domain-level alignment. Looking ahead, we believe that the periodic sampling strategy holds significant potential for enhancing cross-machine fault diagnosis with substantial distributional differences. Furthermore, this strategy offers a new perspective for developing a generalized bearing fault diagnosis method applicable across diverse scenarios.

REFERENCES

- [1] S. Qiu, X. Cui, Z. Ping, N. Shan, Z. Li, X. Bao, and X. Xu, “Deep learning techniques in intelligent fault diagnosis and prognosis for industrial systems: A review,” *Sensors*, 2023.
 - [2] M. Sun, H. Wang, P. Liu, Z. Long, J. Yang, and S. Huang, “A novel data-driven mechanical fault diagnosis method for induction motors using stator current signals,” *IEEE Transactions on Transportation Electrification*, 2022.
 - [3] W. Xie, T. Han, Z. Pei, and M. Xie, “A unified out-of-distribution detection framework for trustworthy prognostics and health management in renewable energy systems,” *Engineering Applications of Artificial Intelligence*, 2023.
 - [4] T. Han, J. Tian, C. Chung, and Y.-M. Wei, “Challenges and opportunities for battery health estimation: Bridging laboratory research and real-world applications,” *Journal of Energy Chemistry*, 2024.
 - [5] J. Wang, Y. Chen, K. Liu, D. Wei, S. Zhou, J. Chen, K. Li, H. Luan, and H. Cai, “Comb filter-based noise cancellation for fast di-agnosis of single-point bearing faults in permanent magnet synchronous machines,” *IEEE Transactions on Transportation Electrification*, 2024.
 - [6] S. Yan, H. Shao, X. Wang, and J. Wang, “Few-shot class-incremental learning for system-level fault diagnosis of wind turbine,” *IEEE/ASME Transactions on Mechatronics*, 2024.
 - [7] Z. Zhao, Q. Zhang, X. Yu, C. Sun, S. Wang, R. Yan, and X. Chen, “Applications of unsupervised deep transfer learning to intelligent fault diagnosis: A survey and comparative study,” *IEEE Transactions on Instrumentation and Measurement*, 2021.
 - [8] F. Lu, Q. Tong, J. Xu, Z. Feng, X. Wang, J. Huo, and Q. Wan, “Towards multi-scene learning: A novel cross-domain adaptation model based on sparse filter for traction motor bearing fault diagnosis in high-speed emu,” *Advanced Engineering Informatics*, 2024.
 - [9] C. He, H. Shi, R. Li, J. Li, and Z. Yu, “Interpretable modulated differentiable stft and physics-informed balanced spectrum metric for freight train wheelset bearing cross-machine transfer fault diagnosis under speed fluctuations,” *arXiv preprint arXiv:2406.11917*, 2024.
 - [10] J. Zhang, K. Zhang, Y. An, H. Luo, and S. Yin, “An integrated multitask intelligent bearing fault diagnosis scheme based on representation learning under imbalanced sample condition,” *IEEE Transactions on Neural Networks and Learning Systems*, 2024.
 - [11] S. Li and J. Yu, “A multisource domain adaptation network for process fault diagnosis under different working conditions,” *IEEE Transactions on Industrial Electronics*, 2022.
 - [12] K. Zhao, H. Jiang, K. Wang, and Z. Pei, “Joint distribution adaptation network with adversarial learning for rolling bearing fault diagnosis,” *Knowledge-Based Systems*, 2021.
 - [13] J. Wang, H. Shao, Y. Peng, and B. Liu, “Psparsesformer: Enhancing fault feature extraction based on parallel sparse self-attention and multiscale broadcast feed-forward block,” *IEEE Internet of Things Journal*, 2024.

- [14] F. Lu, Q. Tong, Z. Feng, and Q. Wan, "Unbalanced bearing fault diagnosis under various speeds based on spectrum alignment and deep transfer convolution neural network," *IEEE Transactions on Industrial Informatics*, 2023.
- [15] X. Zhang, Y. Hu, A. Yin, J. Deng, H. Xu, and J. Si, "Inferable deep distilled attention network for diagnosing multiple motor bearing faults," *IEEE Transactions on Transportation Electrification*, 2022.
- [16] F. Lu, Q. Tong, X. Jiang, Z. Feng, J. Xu, and J. Huo, "Deep multilayer sparse regularization time-varying transfer learning networks with dynamic kullback–leibler divergence weights for mechanical fault diagnosis," *IEEE Transactions on Industrial Informatics*, 2024.
- [17] J. Zheng, C. Yang, F. Zheng, and B. Jiang, "A rolling bearing fault diagnosis method using multi-sensor data and periodic sampling," in *2022 IEEE International Conference on Multimedia and Expo (ICME)*, 2022.
- [18] C. Zhao, E. Zio, and W. Shen, "Domain generalization for cross-domain fault diagnosis: an application-oriented perspective and a benchmark study," *Reliability Engineering & System Safety*, 2024.
- [19] T. Gao, J. Yang, and Q. Tang, "A multi-source domain information fusion network for rotating machinery fault diagnosis under variable operating conditions," *Information Fusion*, 2024.
- [20] Y. Xia, C. Shen, D. Wang, Y. Shen, W. Huang, and Z. Zhu, "Moment matching-based intraclass multisource domain adaptation network for bearing fault diagnosis," *Mechanical Systems and Signal Processing*, 2022.
- [21] A. Gretton, D. Sejdinovic, H. Strathmann, S. Balakrishnan, M. Pontil, K. Fukumizu, and B. K. Sriperumbudur, "Optimal kernel choice for large-scale two-sample tests," *Advances in neural information processing systems*, 2012.
- [22] Z. Wu, H. Jiang, H. Zhu, and X. Wang, "A knowledge dynamic matching unit-guided multi-source domain adaptation network with attention mechanism for rolling bearing fault diagnosis," *Mechanical Systems and Signal Processing*, 2023.
- [23] D. Xu, Y. Li, Y. Song, L. Jia, and Y. Liu, "Ifds: An intelligent fault diagnosis system with multisource unsupervised domain adaptation for different working conditions," *IEEE Transactions on Instrumentation and Measurement*, 2021.
- [24] Y. Yu, H. R. Karimi, P. Shi, R. Peng, and S. Zhao, "A new multi-source information domain adaption network based on domain attributes and features transfer for cross-domain fault diagnosis," *Mechanical Systems and Signal Processing*, 2024.
- [25] W. Cao, Z. Meng, D. Sun, J. Liu, Y. Guan, L. Cao, J. Li, and F. Fan, "A two-stage domain alignment method for multi-source domain fault diagnosis," *Measurement*, 2023.
- [26] Y. Jin, X. Wang, M. Long, and J. Wang, "Minimum class confusion for versatile domain adaptation," in *Computer Vision–ECCV 2020: 16th European Conference, Glasgow, UK, August 23–28, 2020, Proceedings, Part XXI 16*, 2020.
- [27] J. Chen, W. Hu, D. Cao, Z. Zhang, Z. Chen, and F. Blaabjerg, "A meta-learning method for electric machine bearing fault diagnosis under varying working conditions with limited data," *IEEE Transactions on Industrial Informatics*, 2023.
- [28] M. Ghorvei, M. Kavianpour, M. T. Beheshti, and A. Ramezani, "Spatial graph convolutional neural network via structured subdomain adaptation and domain adversarial learning for bearing fault diagnosis," *Neurocomputing*, 2023.
- [29] Y. Zhu, F. Zhuang, and D. Wang, "Aligning domain-specific distribution and classifier for cross-domain classification from multiple sources," in *Proceedings of the AAAI conference on artificial intelligence*, 2019.
- [30] J. Tian, D. Han, M. Li, and P. Shi, "A multi-source information transfer learning method with subdomain adaptation for cross-domain fault diagnosis," *Knowledge-Based Systems*, 2022.

VII. BIOGRAPHY SECTION

Jianbo Zheng received his B.S. degree in Software Engineering from Xiangtan University in 2018 and his M.S. degree in Software Engineering from Central South University in 2021. He is currently pursuing a Ph.D. in the College of Computer Science and Electronic Engineering at Hunan University. Additionally, he is serving as a visiting scholar at Macquarie University.

His research interests primarily focus on the application of advanced machine learning techniques, including deep learning, transfer learning, and reinforcement learning, in the context of anomaly detection.

Chao Yang received the B.S. and M.S. degrees in computer science from Hunan University, China in 1999 and 2005, respectively, and the Ph.D. degree in computational intelligence and systems science from Tokyo Institute of Technology, Japan in 2010. She has ever worked as a postdoctoral researcher at Tokyo Institute of Technology.

Since 2016, she has been an associate professor at the College of Computer Science and Electronic Engineering, Hunan University. Her research interests include natural language understanding, information retrieval and recommendation, and multimedia retrieval and content understanding.

Tairui Zhang received his B.S. degrees in automation from Nanjing Agricultural University in 2020. He is currently working toward the M.S. degree in the College of Computer Science and Electronic Engineering, Hunan University.

His research interests include the application of deep learning, transfer learning and graph neural network in anomaly detection and topology based satellite network fault diagnosis.

Bin Jiang received the B.S. and M.S. degrees from Hunan University, China in 1993 and 2006, respectively, and the Ph.D. degree from Tokyo Institute of Technology, Japan in 2015. Since 2021, he has been a professor at the College of Computer Science and Electronic Engineering, Hunan University, China. His research interests include artificial intelligence, big data technology, computer vision, and machine learning.

Xuhui Fan Xuhui Fan is a lecturer in Artificial Intelligence in the School of Computing at Macquarie University, Australia. He received the bachelor's degree in mathematical statistics from the University of Science and Technology of China in 2010, and the Ph.D. degree in computer science from the University of Technology Sydney, Australia in 2015. He was a project engineer at Data61 (previously NICTA), CSIRO, a postdoc fellow in the School of Mathematics and Statistics at the University of New South Wales, and a lecturer at the University of Newcastle, Australia.

His current research interests include Generative AI, Gaussian processes and their wide applications.

Xiao-Ming Wu is currently a M.S. student in Computer Science and Engineering at Sun Yat-sen University. He obtained his B.S. degree in Software Engineering from Shandong University in 2022. Additionally, he served as a visiting scholar at Macquarie University from June 2024 to December 2024, and this work was mainly done at that time.

His research interests include general deep learning and computer vision algorithms. Currently he is working on Embodied AI, Generative Modeling and Efficient AI.

Haidong Shao (Senior Member, IEEE) received the B.S. degree in Electrical Engineering and Automation and the Ph.D. degree in Vehicle Operation Engineering from Northwestern Polytechnical University, Xi'an, China, in 2013 and 2018, respectively. He is currently an Associate Professor in the College of Mechanical and Vehicle Engineering at Hunan University, Changsha, China. From 2019 to 2021, he was a Postdoctoral Fellow with the Division of Operation and Maintenance Engineering, Luleå University of Technology, Luleå, Sweden. His current research interests include prognostics and health management, intelligent diagnosis and maintenance, multi-source information fusion, and industrial internet.

He won the Highly Cited Researchers (Clarivate Analytics), Highly Cited Chinese Researchers (Elsevier), and World's Top 2% Scientists (Stanford University). He has served as the Associate Editors of *IEEE Transactions on Industrial Informatics*, *IEEE Transactions on Systems, Man, and Cybernetics: Systems*, *IEEE Transactions on Intelligent Transportation Systems*, *IEEE Sensors Journal*, and *Journal of Vibration and Control*.